Supporting information for: Reliable nanometre-range distance distributions from 5-pulse Double Electron Electron Resonance

Frauke D. Breitgoff, Yevhen O. Polyhach, Gunnar Jeschke

1 Zero-time determination

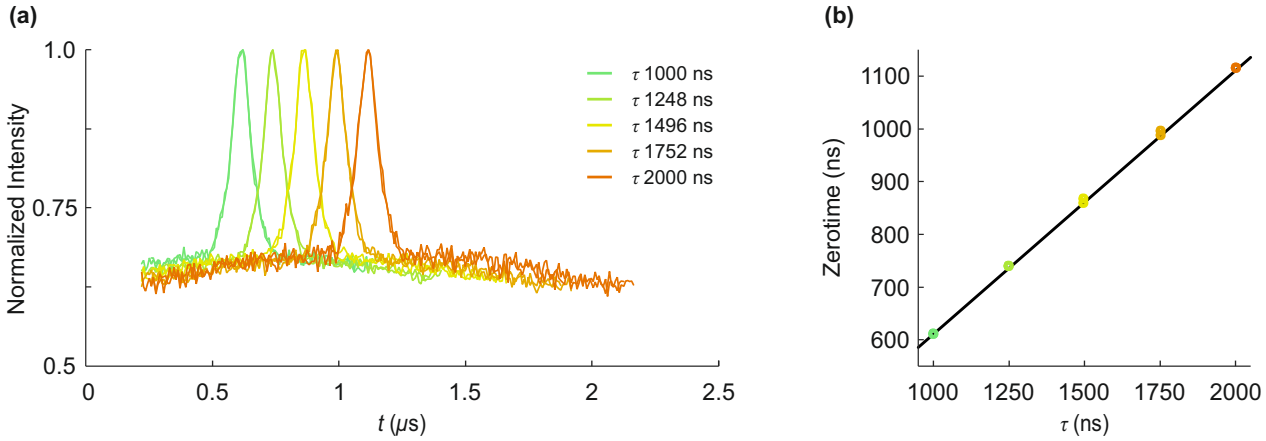

Fig. S1: **(a)** 4-pulse DEER measurements with symmetric (Carr-Purcell) timings of WALP23 (A7R1,W22R1) with various τ. The pump pulse was a 100 ns HS16 pulse with a width of 150 MHz. **(b)** Zero times determined from the symmetric 4-pulse DEER measurements. A linear regression according to $f(\tau) = 0.5 \cdot \tau - 29$ ns is overlaid as black line.

In our hands, the individual determination of the zero time of the partial excitation artefact was not strictly necessary if the zero time of the ideal 5-pulse signal (pathway **1** in Table 1 in the main article) was determined beforehand for a given set of pulse parameters by measuring with a short delay τ, as is common praxis in 4-pulse DEER already. In this case, the zero time of the partial excitation artefact occurs $\tau/2 - t_0$ after the ideal 5-pulse signal.

This can be explained as follows. On the time axis t', where $t' = 0$ at the first refocusing observer π-pulse (see Figure 1 in main article), the zero time of the ideal 5-pulse signal is $t' = t_0 + z_5$, where z_5 is the time-shift of the ideal 5-pulse signal due to non-zero pulse lengths. On the same time axis t', the zero time of the partial excitation artefact is $t' = \tau/2 + z_4$. Here, z_4 is the time-shift of the partial excitation artefact due to non-zero pulse lengths. If we assume that $z = z_5 = z_4$, then the time shift z cancels in the difference of the two timings and the partial excitation artefact occurs $\tau/2 - t_0$ after the ideal 5-pulse signal. The time shift

z is expected to be independent of τ, and in the range for which we tested this assumption (Fig. S1b) indeed zero times shifted linearly, according to $f(\tau) = 0.5 \cdot \tau + z$.

The best results in our hands were obtained if the zero time of the ideal 5-pulse signal and the zero time of the partial excitation artefact relative to the ideal 5-pulse signal were fixed as $t' + z_5$ and $\tau/2 - t_0 + z_4 - z_5$, respectively. However, accuracy of artefact correction already improved if just the zero time of the partial excitation artefact relative to the ideal 5-pulse signal was set to $\tau/2 - t_0$ and the zero time of the ideal 5-pulse signal ($t' + z$) was found by the algorithm.

2 Artefact correction for bimodal distributions

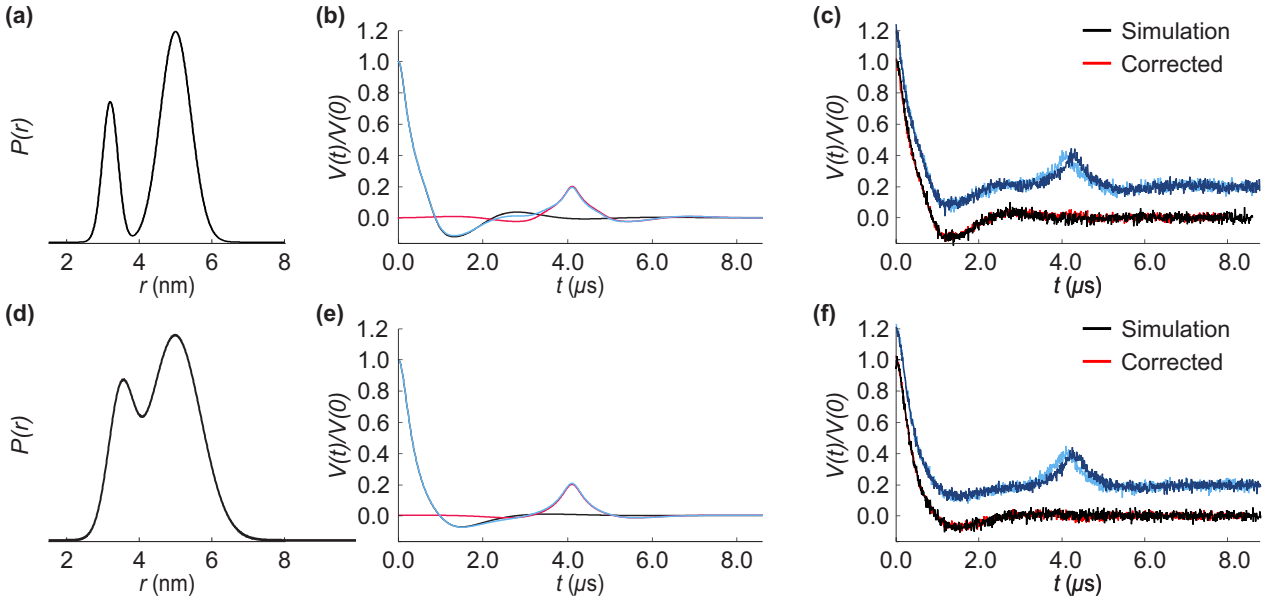

Fig. S2: Comparison of corrected 5-pulse DEER dipolar evolution functions simulated for distance distributions shown on the left to simulated pure 5-pulse signal. **(a,d)** Distance distribution, **(b,e)** Simulated 5-pulse DEER trace (blue) containing the partial excitation artefact with an intensity of 20% (red), **(c,f)** Comparison of the two traces simulated with slightly different t_0 and noise added (light and dark blue), corrected traces (red) and pure 5-pulse signal (black).

3 Distance extraction without accounting for the artefact

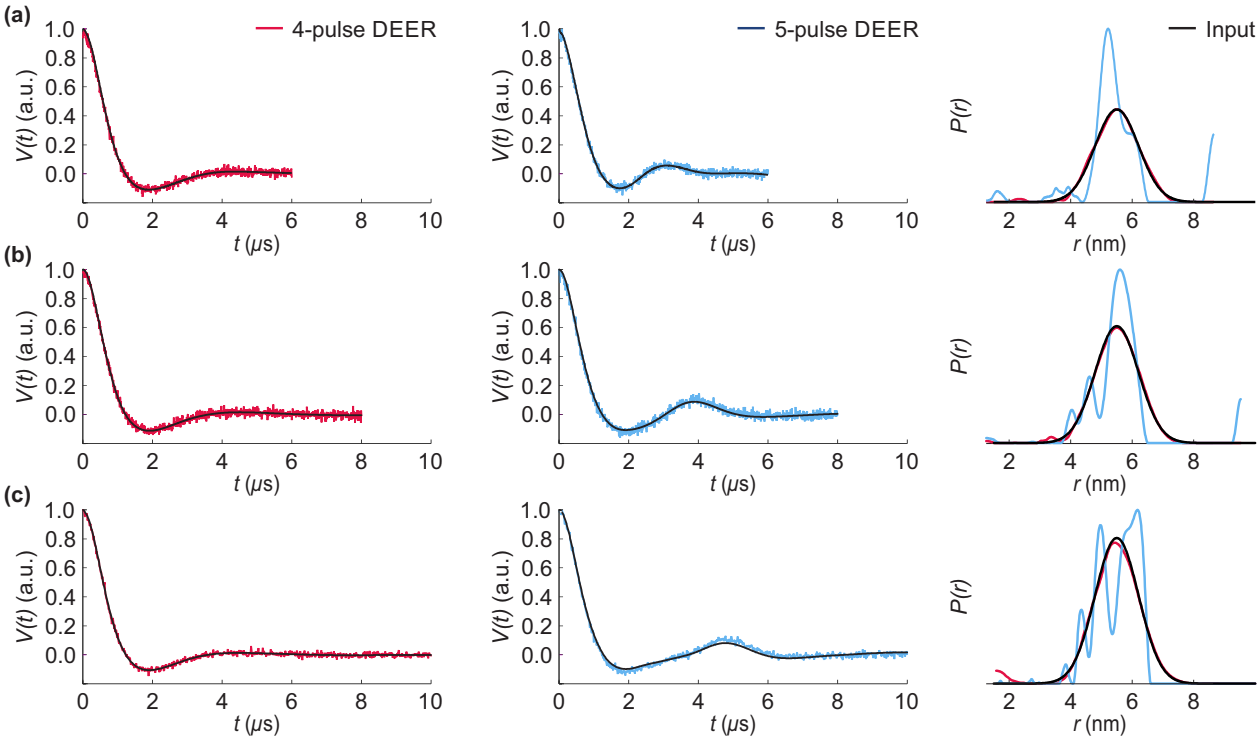

Fig. S3: DEER dipolar evolution functions simulated for a Gaussian distance distribution ($r_{mean} = 5.5$ nm, $\sigma = 1$ nm) and different dipolar evolution times (red). The partial excitation artefact was included with an intensity of 10% for the simulation of 5-pulse DEER traces (blue). Fits (black) and extracted distance distributions by DeerAnalysis[1] without prior artefact removal are shown with the regularization parameter selected by L-curve criterion. Depending on the ratio of τ to the period of dipolar oscillation in the 5-pulse DEER traces, different distortions of the extracted distance distribution are observed. **(a)** $\tau = 6$ μs, **(b)** $\tau = 8$ μs, **(c)** $\tau = 10$ μs.

4 Structures of the rigid biradicals

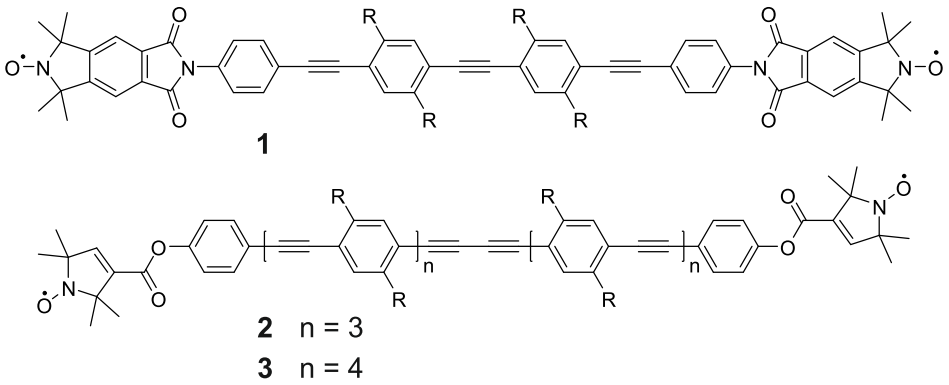

Fig. S4: Structures of the rigid biradicals [2]. R is a 6-methoxyhexyl substituent for **1** and a hexyl substituent for **2** and **3**.

5 Artefact correction for a biradical with broad distance distribution and strong background decay

The rigid model biradical **3** (Fig. S4) was synthesized to have a narrowly distributed inter-spin distance of ca. 8 nm [2]. Due to very long storage time, the sample has undergone some degradation resulting in appearance of the additional broad shorter-distance band and strong background decay, Fig. S5, (compare [2]). Because of these features and due to the fact that the artefact signal is not fully decayed at the end of the trace, this sample constituted an interesting challenge for the artefact removal procedure. Still, the frequency content of the artefact-corrected 5-pulse DEER trace is similar to that of 4-pulse DEER data and a very similar distance distribution is extracted.

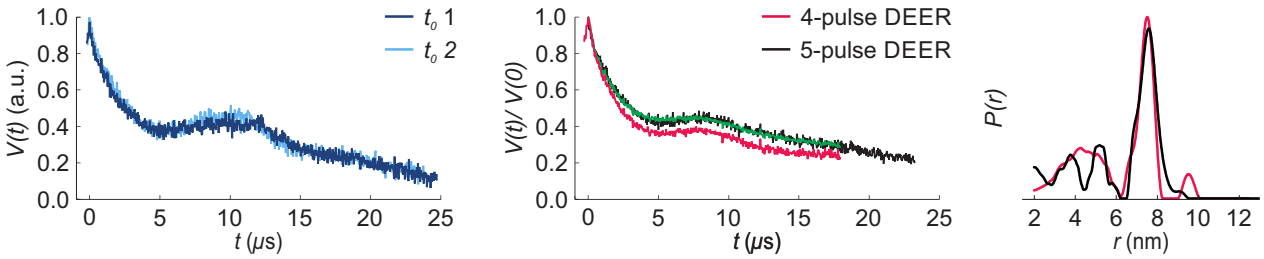

Fig. S5: Artefact correction for rigid biradical **3** in *d*-OTP ($n = 4$), $\Delta\, t_0 = 792$ ns. Left: raw 5-pulse DEER traces measured with two different t_0 values; Middle: artefact corrected 5-pulse DEER (black) compared to 4-pulse DEER (red), 4-pulse DEER also shown with background parameters adopted to match 5-pulse trace (green); Right: distance distributions extracted by Tikhonov regularization [1].

6 Artefact correction for short traces

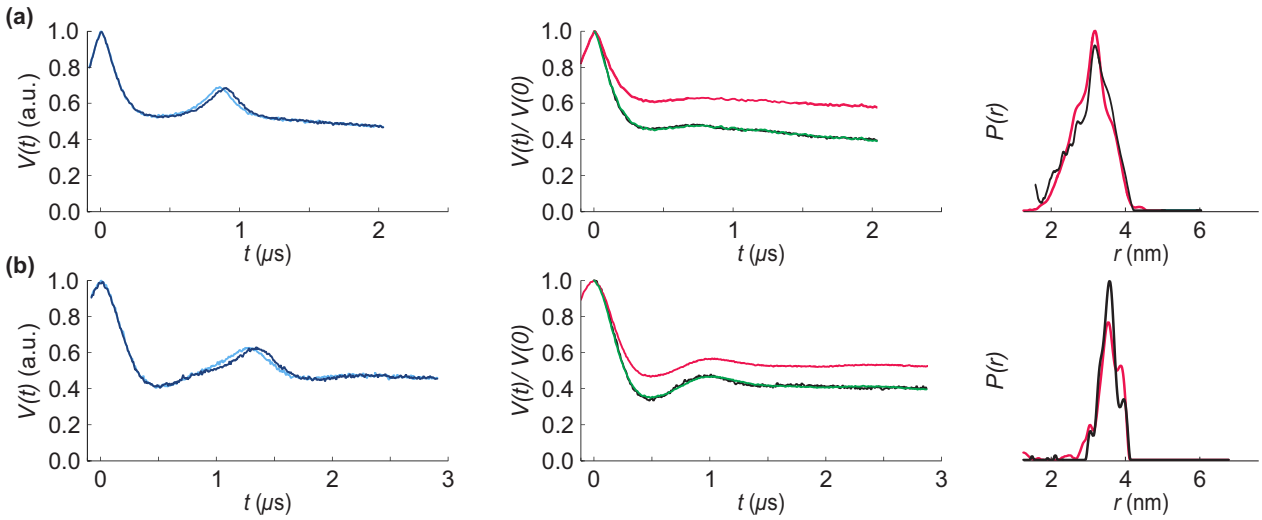

Fig. S6: Artefact correction for traces that are measured short with respect to the dipolar oscillation period. **(a)** WALP23 (W2R1/W22R1), $\Delta\ t_0 = 40$ ns, **(b)** T4L lysozyme (C72R1/C131R1), $\Delta\ t_0 = 56$ ns.

References

(1) G. Jeschke, V. Chechik, P. Ionita, A. Godt, H. Zimmermann, J. Banham, C. R. Timmel, D. Hilger and H. Jung, *Appl. Magn. Reson.*, 2006, **30**, 473–498.

(2) G. Jeschke, M. Sajid, M. Schulte, N. Ramezanian, A. Volkov, H. Zimmermann and A. Godt, *J. Am. Chem. Soc.*, 2010, **132**, 10107–10117.